

Microscopic derivation of transport coefficients and boundary conditions in discrete drift-diffusion models of weakly coupled superlattices

L. L. Bonilla

Departamento de Matemáticas, Escuela Politécnica Superior, Universidad Carlos III de Madrid, Avenida de la Universidad 30, 28911 Leganés, Spain
and Unidad Asociada al Instituto de Ciencia de Materiales (CSIC)

G. Platero and D. Sánchez

Instituto de Ciencia de Materiales (CSIC), Cantoblanco, 28049 Madrid, Spain
 (Received 29 September 1999; revised manuscript received 2 February 2000)

A discrete drift-diffusion model is derived from a microscopic sequential tunneling model of charge transport in weakly-coupled superlattices provided temperatures are low or high enough. Realistic transport coefficients and contact current-field characteristic curves are calculated from microscopic expressions, knowing the design parameters of the superlattice. Boundary conditions clarify when possible self-sustained oscillations of the current are due to monopole or dipole recycling.

I. INTRODUCTION

At present, the theory of charge transport and pattern formation in superlattices (SL) is in a fragmentary state. On the one hand, it is possible to establish a quantum kinetic theory from first principles by using Green-function formalisms.^{1,2} However, the resulting equations are hard to solve, even numerically, unless a number of simplifications and assumptions are made.^{2,3} These include: (i) a constant electric field, (ii) simplified scattering models, and (iii) a stationary current through the SL. These assumptions directly exclude the description of electric-field domains and their dynamics although important results are still obtained.^{3,4} The stationary current density probes the difference between strongly- and weakly-coupled SL. It also indicates when simpler theories yield good agreement with quantum kinetics. The main simpler theories are (see Fig. 1 of Ref. 3):

(i) Semiclassical calculations of miniband transport using the Boltzmann transport equation⁵ or simplifications thereof, such as hydrodynamic⁶ or drift-diffusion⁷ models. These calculations hold for strongly coupled SL at low fields. In the miniband transport regime, electrons traverse the whole SL miniband thereby performing Bloch oscillations and giving rise to negative differential conductivity for large enough electric fields.⁸ The latter may cause self-sustained oscillations of the current due to recycling of charge dipole domains as in the Gunn effect of bulk *n*-GaAs.^{9,6}

(ii) Wannier-Stark (WS) hopping transport in which electrons move parallel to the electric field through scattering processes including hopping transitions between WS levels.¹⁰ Calculations in this regime hold for intermediate fields, larger than those corresponding to collisional broadening of WS levels, but lower than those corresponding to resonant tunneling.

(iii) Sequential tunneling calculations valid for weakly-coupled SL (coherence length smaller than one SL period) at basically any value of the electric field.¹¹⁻¹³ A great advantage of this formulation as compared with (i), (ii) or Green's-function calculations is that boundary conditions can be de-

rived naturally and consistently from microscopic models.¹²

On the other hand, the description of electric-field domains and self-sustained oscillations in SL has been made by means of discrete drift models. These models use simplified forms of the tunneling current through SL barriers and discrete forms of the charge continuity and Poisson equations.¹⁴⁻¹⁶ Although discrete drift models yield good descriptions of nonlinear phenomena in SL, bridging the gap between them and more microscopic descriptions^{12,13} is greatly desirable for further advancing both theory and experiments.

A step in this direction is attempted in the present paper. Our starting point is a microscopic description of a weakly-coupled SL by means of discrete Poisson and charge continuity equations. In the latter the tunneling current through a barrier is a function of the electrochemical potentials of adjacent wells and the potential drops in them and in the barrier. This function is derived by means of the transfer Hamiltonian method provided the intersubband scattering and the

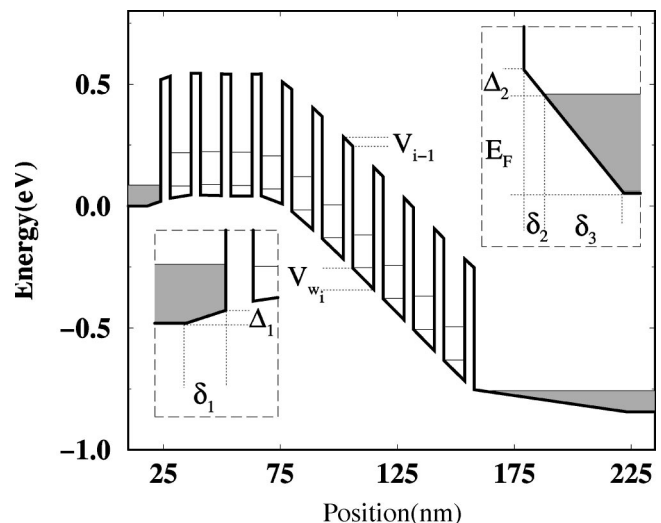


FIG. 1. Sketch of the electrostatic potential profile in a SL.

tunneling time are much smaller than the typical dielectric relaxation time.¹² From this microscopic model and for sufficiently low or high temperatures, we derive discrete drift-diffusion (DDD) equations for the field and charge at each SL period and appropriate boundary conditions. The drift velocity and diffusion coefficients in the DDD equations are nonlinear functions of the electric field that can be calculated from first principles for any weakly coupled SL. These equations are of great interest for the study of nonlinear dynamics in SL. They are simpler to study than microscopic model equations for which only numerical simulation results are available.¹⁸

In the present paper, natural boundary conditions for DDD equations are derived from microscopic calculations for the first time. Previous authors had to propose boundary conditions with adjustable parameters that gave qualitative agreement with experimental results.^{13–17} The present boundary conditions relate current density and field at contacts and can be calculated for a given configuration of emitter and collector contact regions. As it is well-known, boundary conditions select the stable charge and field profiles in the SL, and therefore are crucial to understand which spatiotemporal structures will be observed in the SL for given values of the control parameters.^{13–17}

The rest of the paper is as follows. In Sec. II, we review the microscopic sequential resonant tunneling model. We obtain the minimal set of independent equations and boundary conditions describing this model. Our derivation of the DDD model is presented in Sec. III. Numerical evaluation of ve-

locity, diffusion, and contact coefficients for several SL's is presented in Sec. IV. Section V contains our conclusions. The appendix contains an evaluation of the transport coefficients for negative values of the electric field.

II. MICROSCOPIC SEQUENTIAL TUNNELING MODEL

The main charge transport mechanism in a weakly-coupled SL is sequential resonant tunneling. We shall assume that the macroscopic time scale of the self-sustained oscillations is larger than the tunneling time (defined as the time an electron needs to advance from one well to the next one). In turn, this latter time is supposed to be much larger than the intersubband scattering time. This means that we can assume the process of tunneling across a barrier to be stationary, with well-defined Fermi-Dirac distributions at each well, which depend on the instantaneous values of the electron density and potential drops. These densities and potentials vary only on the longer macroscopic time scale.

A. Tunneling current

The tunneling current density across each barrier in the SL may be approximately calculated by means of the transfer Hamiltonian method. We shall only quote the results here.¹² Let $eJ_{e,1}$ and $eJ_{N,c}$ be the currents in the emitter and collector contacts, respectively, and let $eJ_{i,i+1}$ be the current through the i th barrier which separates wells i and $i+1$. We have

$$J_{e,1} \equiv J_{0,1} = \frac{k_B T}{2\pi^2 \hbar} \sum_{j=1}^n \int A_{Cj}^1(\epsilon) B_{0,1}(\epsilon) T_0(\epsilon) \ln \left[\frac{1 + e^{(\epsilon_F - \epsilon)/k_B T}}{1 + e^{\epsilon_{w_1} - \epsilon/k_B T}} \right] d\epsilon, \quad (1)$$

$$J_{i,i+1} = \frac{\hbar k_B T}{2\pi^2 m^*} \sum_{j=1}^n \int A_{C1}^i(\epsilon) A_{Cj}^{i+1}(\epsilon) B_{i-1,i}(\epsilon) B_{i,i+1}(\epsilon) T_i(\epsilon) \ln \left[\frac{1 + e^{(\epsilon_{w_i} - \epsilon)/k_B T}}{1 + e^{\epsilon_{w_{i+1}} - \epsilon/k_B T}} \right] d\epsilon, \quad (2)$$

$$J_{N,c} \equiv J_{N,N+1} = \frac{k_B T}{2\pi^2 \hbar} \int A_{C1}^N(\epsilon) B_{N-1,N}(\epsilon) T_N(\epsilon) \ln \left[\frac{1 + e^{(\epsilon_{w_N} - \epsilon)/k_B T}}{1 + e^{(\epsilon_F - eV - \epsilon)/k_B T}} \right] d\epsilon. \quad (3)$$

In these expressions:

(1) $i = 1, \dots, N-1$, n is the number of subbands in each well i with energies ϵ_{Cj}^i (measured with respect to the common origin of potential drops: $\epsilon = 0$ at the bottom of the emitter conduction band). $\epsilon_F = \hbar^2 (3\pi^2 N_D)^{2/3} / (2m_w^*)$ are the Fermi energies of the emitter and collector regions calculated as functions of their doping density N_D . m_w^* and m^* are the effective masses of the electrons at the wells and barriers, respectively.

(2) $B_{i-1,i}$ are given by

$$B_{i-1,i} = k_i \left[w + \left(\frac{1}{\alpha_{i-1}} + \frac{1}{\alpha_i} \right) \left(\frac{m^*}{m_w^*} \sin^2 \frac{k_i w}{2} + \cos^2 \frac{k_i w}{2} \right) \right]^{-1}, \quad (4)$$

$$\hbar k_i = \sqrt{2m_w^* (\epsilon + eW_i)}, \quad (5)$$

$$\hbar \alpha_i = \sqrt{2m^* e \left[V_b - W_i - \frac{V_{w_i}}{2} - \frac{\epsilon}{e} \right]}, \quad (6)$$

$$W_i \equiv \sum_{j=0}^{i-1} (V_j + V_{w_j}) + \frac{V_{w_i}}{2}, \quad (7)$$

where k_i and α_i are the wave vectors in the wells and the barriers, respectively. k_i depends on the electric potential at the center of the i th well W_i , whereas α_i depends on the potential at the beginning of the i th barrier $W_i + V_{w_i}/2$. See Fig. 1. V_i and V_{w_i} , $i = 1, \dots, N$, are the potential drops at the i th barrier and well, respectively. We assume that the potential drops at barrier and wells are non-negative and that the electrons are singularly concentrated on a plane located at the end of each well (which is consistent with the choice of

α_i ; the choice of k_i is dictated by the transfer Hamiltonian method). The potential drops V_0 and V_N correspond to the barriers separating the SL from the emitter and collector contacts, respectively. $\Delta_1 \equiv eV_{w_0} = 2eW_0$ is the energy drop at the emitter region, and eV_b is the barrier height in the absence of potential drops.

(3) T_i is the dimensionless transmission probability through the i th barrier separating wells i and $i+1$:

$$T_i(\epsilon) = \frac{16k_i k_{i+1} \alpha_i^2 e^{-2\alpha_i d}}{\left[k_i^2 + \left(\frac{m_w^* \alpha_i}{m^*} \right)^2 \right] \left[k_{i+1}^2 + \left(\frac{m_w^* \alpha_i}{m^*} \right)^2 \right]}, \quad (8)$$

provided $\alpha_i d \gg 1$.

(4) w and d are the widths of wells and barriers, respectively.

(5) Scattering is included in our model by means of Lorentzian functions:

$$A_{C_j}^i(\epsilon) = \frac{\gamma}{(\epsilon - \epsilon_{C_j}^i)^2 + \gamma^2} \quad (9)$$

(for the i th well). The Lorentzian half-width is $\gamma = \hbar/\tau_{sc}$, where τ_{sc} is the lifetime associated to any scattering process dominant in the sample (interface roughness, impurity scattering, phonon scattering, . . .).^{19–22} For the samples considered here, γ ranges from 1 to 10 meV.¹⁷ Of course this phenomenological treatment of scattering could be improved by calculating microscopically the self-energy associated to one of the scattering processes mentioned above. However this restriction to one scattering mechanism would result in a loss of generality and simplicity of the model.

(6) The integration variable ϵ takes on values from the bottom of the i th well to infinity.

Of course this model can be improved by calculating microscopically the self-energies, which could include other scattering mechanisms (e.g., interface roughness, impurity effects^{4,13}) or even exchange-correlation effects (which affect the electron charge distribution in a self-consistent way). We have assumed that the electrons at each well are in local equilibrium with Fermi energies ϵ_{w_i} , which define the electron number densities n_i :

$$n_i(\epsilon_{w_i}) = \frac{m_w^* k_B T}{\pi^2 \hbar^2} \int A_{C_1}^i(\epsilon) \ln[1 + e^{(\epsilon_{w_i} - \epsilon)/k_B T}] d\epsilon. \quad (10)$$

Notice that the complicated dependence of the wave vectors k_i and α_i with the potential, W_i , may be transferred to the Fermi energies by changing variables in the integrals of the system (2) so that the lower limit of integration (the bottom of the i th well) is zero: $\epsilon' = \epsilon + eW_i$. Then the resulting expressions have the same forms as Eqs. (2) and (10) if $\epsilon_{C_1}^i$, $\epsilon_{C_j}^{i+1}$, and ϵ_{w_i} in them are replaced by

$$\epsilon_{C_1} = \epsilon_{C_1}^i + eW_i, \quad (11)$$

$$\mu_i \equiv \epsilon_{w_i} + eW_i, \quad (12)$$

respectively. W_i is given by Eq. (7). The integrations now go from $\epsilon' = 0$ to infinity. Notice that ϵ_{C_j} is independent of the well index i provided we assume that the energy level drops half of the potential drop for the whole well eV_{w_i} with respect to its position in the absence of bias. Equation (10) becomes

$$n_i(\mu_i) = \frac{m_w^* k_B T}{\pi^2 \hbar^2} \int_0^\infty A_{C_1}(\epsilon) \ln[1 + e^{(\mu_i - \epsilon)/k_B T}] d\epsilon. \quad (13)$$

Here $A_{C_1}(\epsilon)$ is obtained by substituting ϵ_{C_1} (the energy of the first subband measured from the bottom of a given well, therefore independent of electrostatics) instead of $\epsilon_{C_1}^i$ in Eq. (9). Notice that Eq. (13) defines a one-to-one relation between n_i and μ_i that is independent of the index i or the potential drops. The inverse function

$$\mu_i = \mu(n_i, T)$$

gives the chemical potential or free energy per electron. This is the *entropic* part of the electrochemical potential (Fermi energy)

$$\epsilon_{w_i} = \mu(n_i, T) - e \sum_{j=0}^{i-1} (V_j + V_{w_j}) - \frac{eV_{w_i}}{2}. \quad (14)$$

According to Eq. (14), the Fermi energy ϵ_{w_i} (electrochemical potential) is the sum of the electrostatic energy at the i th well,

$$-e \sum_{j=0}^{i-1} (V_j + V_{w_j}) - eV_{w_i}/2,$$

and the chemical potential $\mu_i = \mu(n_i, T)$.

After the change of variable in the integrals, the wave vectors in Eq. (2) become

$$\begin{aligned} \hbar k_i &= \sqrt{2m_w^* \epsilon}, \\ \hbar \alpha_i &= \sqrt{2m_w^* \left(eV_b - \frac{eV_{w_i}}{2} - \epsilon \right)}, \\ \hbar k_{i+1} &= \sqrt{2m_w^* \left(\epsilon + eV_i + e \frac{V_{w_i} + V_{w_{i+1}}}{2} \right)}, \\ \hbar \alpha_{i-1} &= \sqrt{2m_w^* \left(eV_b + \frac{eV_{w_i}}{2} + eV_{i-1} - \epsilon \right)}, \\ \hbar \alpha_{i+1} &= \sqrt{2m_w^* \left(eV_b - \frac{eV_{w_i}}{2} - eV_i - eV_{w_{i+1}} - \epsilon \right)}, \end{aligned} \quad (15)$$

where now $\epsilon = 0$ at the bottom of the i th well. This shows that the tunneling current density $J_{i,i+1}$ in Eq. (2) is a function of the temperature, μ_i and μ_{i+1} (therefore of n_i and n_{i+1}), and the potential drops V_i , V_{i+1} , V_{w_i} , and $V_{w_{i+1}}$:

$$J_{i,i+1} = \tilde{\Xi}(n_i, n_{i+1}, V_i, V_{i+1}, V_{w_i}, V_{w_{i+1}}). \quad (16)$$

Similarly, we have

$$J_{e,1} = \tilde{\Xi}_e(n_1, N_D, V_0, V_{w_1}), \quad (17)$$

$$J_{N,c} = \tilde{\Xi}_c(n_N, N_D, V_N, V_{w_N}). \quad (18)$$

B. Balance and Poisson equations

The two-dimensional (2D) electron densities evolve according to the following rate equations:

$$\frac{dn_i}{dt} = J_{i-1,i} - J_{i,i+1}, \quad i = 1, \dots, N. \quad (19)$$

The voltage drops through the structure are calculated as follows. The Poisson equation yields the potential drops in the barriers V_i , and the wells V_{w_i} (see Fig. 1):

$$\varepsilon_w \frac{V_{w_i}}{w} = \varepsilon \frac{V_{i-1}}{d} + \frac{e(n_i - N_D^w)}{2}, \quad (20)$$

$$\frac{V_i}{d} = \frac{V_{i-1}}{d} + \frac{e(n_i - N_D^w)}{\varepsilon}, \quad (21)$$

where ε_w and ε are the GaAs and AlAs static permittivities respectively, n_i is the 2D (areal) electron number density (to be determined) which is singularly concentrated on a plane located at the end of the i th well, and N_D^w is the 2D intentional doping at the wells.

C. Boundary conditions

The emitter and collector layers can be described by the following equations:

$$\frac{\varepsilon_w \Delta_1}{\delta_1} = \frac{\varepsilon e V_0}{d}, \quad \sigma_e = 2\varepsilon \frac{V_0}{d} \approx eN(\varepsilon_F) \Delta_1 \delta_1, \quad (22)$$

$$\frac{\varepsilon_w \Delta_2}{e \delta_2} = \frac{\varepsilon V_N}{d} - \frac{e N_D \delta_2}{2} = \frac{\varepsilon_w \varepsilon_F}{e \delta_3}, \quad (23)$$

$$\sigma_c = 2\varepsilon_w \frac{\varepsilon_F}{e \delta_3} = e N_D \left(\delta_2 + \frac{1}{2} \delta_3 \right). \quad (24)$$

To write the emitter equations (22), we assume that there are no charges in the emitter barrier.²³ Then the electric field across δ_1 (see Fig. 1) is equal to that in the emitter barrier. Furthermore, the areal charge density σ_e required to create this electric field is provided by the emitter. $N(\varepsilon_F) = m_w^* \hbar^{-2} (3N_D / \pi^4)^{1/3}$ is the density-of-states at the emitter Fermi energy $\varepsilon_F = \hbar^2 (3\pi^2 N_D)^{2/3} / (2m_w^*)$. The collector equations (23) and (24) ensure that the electrons tunneling through the N th (last) barrier are captured by the collector. They hold if the bias is large enough (see below). We assume that: (i) the region of length δ_2 in the collector is completely depleted of electrons, (ii) there is local charge neutrality in the region of length δ_3 between the end of the depletion layer δ_2 and the collector, and (iii) the areal charge density σ_c required to create the local electric field is supplied by the collector. Notice that $eN_D(\delta_2 + \frac{1}{2}\delta_3)$ in Eq. (24) is the positive 2D charge density depleted in the collector region. Equations (23) and (24) hold provided $V_N \geq \varepsilon_w \varepsilon_F d / (e\varepsilon \delta_3)$, $\Delta_2 \geq 0$, $\delta_2 \geq 0$, and $\delta_3 \geq 0$. For smaller biases resulting in

$V_N < \varepsilon_w \varepsilon_F d / (e\varepsilon \delta_3)$, a boundary condition similar to Eq. (22) should be used instead of Eqs. (23) and (24):

$$\frac{\varepsilon_w \tilde{\Delta}_2}{\tilde{\delta}_2} = \frac{\varepsilon e V_N}{d}, \quad \sigma_c = 2\varepsilon \frac{V_N}{d} \approx eN(\varepsilon_F) \tilde{\Delta}_2 \tilde{\delta}_2. \quad (25)$$

Notice that $\tilde{\Delta}_2$ and $\tilde{\delta}_2$ have different meanings from Δ_2 and δ_2 in Eq. (23).

The condition of overall voltage bias closes the set of equations:

$$V = \sum_{i=0}^N V_i + \sum_{i=1}^N V_{w_i} + \frac{\Delta_1 + \Delta_2 + \varepsilon_F}{e}. \quad (26)$$

This condition holds only if $V_N \geq \varepsilon_w \varepsilon_F d / (e\varepsilon \delta_3)$; otherwise $(\Delta_2 + \varepsilon_F)$ should be replaced by $\tilde{\Delta}_2$ in Eq. (26).

Notice that we can find δ_1 and Δ_1 as functions of V_0 from Eq. (22):

$$\begin{aligned} \Delta_1 = 0 = V_0, \quad \delta_1 \text{ indetermined or} \\ \delta_1 = \sqrt{\frac{2\varepsilon_w}{e^2 N(\varepsilon_F)}} = \frac{\hbar \pi^{2/3} (2\varepsilon_w)^{1/2}}{em_w^*{}^{1/2} (3N_D)^{1/6}}, \quad \Delta_1 = \frac{e\varepsilon V_0 \delta_1}{\varepsilon_w d}. \end{aligned} \quad (27)$$

Similarly we can find δ_3 by solving Eqs. (23) and (24) in terms of V_N and N_D . From this equation and Eq. (23), we can find δ_2 and Δ_2 as functions of V_N :

$$\begin{aligned} \delta_3 = \frac{2\varepsilon}{eN_D d} \left[\sqrt{V_N^2 + (2\varepsilon_w \varepsilon_F N_D d^2) / \varepsilon^2} - V_N \right], \\ \delta_2 = \frac{2\varepsilon_w \varepsilon_F}{e^2 N_D \delta_3} \left(\frac{eV_N \delta_3 \varepsilon}{\varepsilon_w \varepsilon_F d} - 1 \right) \theta \left(\frac{e\varepsilon V_N \delta_3}{\varepsilon_w \varepsilon_F d} - 1 \right), \\ \Delta_2 = \frac{2\varepsilon \varepsilon_F^2}{e^2 N_D \delta_3^2} \left(\frac{e\varepsilon V_N \delta_3}{\varepsilon_w \varepsilon_F d} - 1 \right) \theta \left(\frac{e\varepsilon V_N \delta_3}{\varepsilon_w \varepsilon_F d} - 1 \right), \end{aligned} \quad (28)$$

where $\theta(x)$ is the Heaviside unit step function. The boundary conditions (23) and (24) do not hold if $e\varepsilon V_N \delta_3 < \varepsilon_w \varepsilon_F d$. This occurs if $V_N < (3\pi^2)^{1/3} N_D^{5/6} \hbar d \sqrt{\varepsilon_w} / [2\varepsilon \sqrt{2m_w^*}]$. In this case, we should impose the alternative boundary conditions (25). From these, we obtain

$$\begin{aligned} \tilde{\delta}_2 = \sqrt{\frac{2\varepsilon_w}{e^2 N(\varepsilon_F)}} = \frac{\hbar \pi^{2/3} (2\varepsilon_w)^{1/2}}{em_w^*{}^{1/2} (3N_D)^{1/6}}, \\ \tilde{\Delta}_2 = \frac{e\varepsilon V_N \tilde{\delta}_2}{\varepsilon_w d} \theta \left(1 - \frac{e\varepsilon V_N \delta_3}{\varepsilon_w \varepsilon_F d} \right). \end{aligned} \quad (29)$$

The critical potential $V_N = \varepsilon_w \varepsilon_F d / (e\varepsilon \delta_3)$ corresponds to $V_N = \varepsilon_w \varepsilon_F d / (\sqrt{3} e\varepsilon \tilde{\delta}_2)$. There is a small mismatch between Eqs. (28) and (29) at this critical potential: $e\varepsilon V_N / d = \varepsilon_w \varepsilon_F / \delta_3$, but $e\varepsilon V_N / d \neq \varepsilon_w \varepsilon_F / \tilde{\delta}_2$. This imperfection can be fixed by using a more precise relation between the charge at the collector σ_c , $\tilde{\Delta}_2$, and $\tilde{\delta}_2$, but we choose not to delve more in these details. In all cases, we have shown that the potential drops at the barriers separating the SL from the contact regions uniquely determine the contact electrostatics.

In Ref. 12 global charge conservation

$$\sigma_e + \sum_{i=1}^N (n_i - eN_D^w) = eN_D(\delta_2 + \frac{1}{2}\delta_3) \quad (30)$$

was used instead of Eq. (24) [which is a condition similar to the one we impose at the emitter contact, Eq. (22)]. Substitution of Eq. (24) instead of Eq. (30) modifies minimally the numerical results reported in Refs. 12 and 18.

D. Elimination of the potential drops at the wells

The previous model has too many equations. We can eliminate the potential drops at the wells from the system. For Eqs. (20) and (21) imply

$$\frac{\varepsilon_w V_{w_i}}{\varepsilon w} = \frac{V_{i-1} + V_i}{2d}. \quad (31)$$

Then the bias condition (26) becomes

$$V = \left(1 + \frac{\varepsilon w}{\varepsilon_w d}\right) \sum_{i=0}^N V_i - \frac{\varepsilon(V_0 + V_N)w}{2\varepsilon_w d} + \frac{\Delta_1 + \Delta_2 + \epsilon_F}{e}, \quad (32)$$

where $\Delta_1 = \Delta_1(V_0)$ and $\Delta_2 = \Delta_2(V_N)$. Instead of the rate equations (19), we can derive a form of Ampère's law that explicitly contains the total current density $J(t)$. We differentiate Eq. (21) with respect to time and eliminate n_i by using Eq. (19). The result is

$$\frac{\varepsilon}{ed} \frac{dV_i}{dt} + J_{i,i+1} = J(t), \quad i = 0, 1, \dots, N, \quad (33)$$

where $eJ(t)$ is the sum of displacement and tunneling currents. The time-dependent model consists of the $2N+2$ equations (21), (32), and (33) [the currents are given by Eqs. (2), (10), (27), (28), and (31)], which contain the $2N+2$ unknowns n_i ($j=1, \dots, N$), V_j ($j=0, 1, \dots, N$), and J . Thus we have a system of equations which, together with appropriate initial conditions, determine completely and self-consistently our problem. For convenience, let us list again the minimal set of equations we need to solve in order to determine completely all the unknowns:

$$\frac{\varepsilon}{ed} \frac{dV_i}{dt} + J_{i,i+1} = J(t), \quad i = 0, 1, \dots, N,$$

$$\frac{V_i}{d} = \frac{V_{i-1}}{d} + \frac{e(n_i - N_D^w)}{\varepsilon}, \quad i = 1, \dots, N, \quad (34)$$

$$V = \left(1 + \frac{\varepsilon w}{\varepsilon_w d}\right) \sum_{i=0}^N V_i - \frac{(V_0 + V_N)\varepsilon w}{2\varepsilon_w d} + \frac{\Delta_1(V_0) + \Delta_2(V_N) + \epsilon_F}{e}, \quad (35)$$

$$J_{i,i+1} = \Xi(n_i, n_{i+1}, V_{i-1}, V_i, V_{i+1}), \quad (36)$$

$$J_{e,1} = \Xi_e(n_1, V_0, V_1), \quad (37)$$

$$J_{N,c} = \Xi_c(n_N, V_{N-1}, V_N). \quad (38)$$

Notice that the three last equations are constitutive relations obtained by substituting Eq. (31) in the functions Ξ , Ξ_e , and Ξ_c of Eqs. (16), (17), and (18), respectively. The functions $\Delta_1(V_0)$ and $\Delta_2(V_N)$ are given by Eqs. (27) and (28), respectively. Equations (33) for $i=0, N$ may be considered the real boundary conditions for the barriers separating the SL from the contacts. These boundary conditions are the balance of current density including special tunneling current constitutive relations $J_{e,1}$ and $J_{N,c}$. The latter depend on the electron densities at the extreme wells of the SL and the potential drops at the adjacent barriers.

III. DERIVATION OF THE DISCRETE DRIFT-DIFFUSION MODEL

It is interesting to consider the relation (10) between the chemical potential and the electron density at a well for different temperature ranges:

$$n_i(\mu_i) = \frac{m_w^* k_B T}{\pi^2 \hbar^2} \int A_{C1}(\epsilon) \ln \left[1 + e^{\frac{\mu_i - \epsilon}{k_B T}} \right] d\epsilon.$$

Assuming that $\mu_i \gg k_B T$, we may approximate this expression by

$$n_i(\mu_i) \approx \frac{m_w^*}{\pi^2 \hbar^2} \int_0^{\mu_i} A_{C1}(\epsilon) (\mu_i - \epsilon) d\epsilon. \quad (39)$$

Thus n_i approaches a linear function of μ_i if $\mu_i \gg k_B T$. For the SL used in the experiments we have been referring to, $\mu_i - \epsilon$ is typically about 20 meV or 232 K. Thus ‘‘low temperature’’ can be ‘‘high enough temperature’’ in practice. Provided the Lorentzian A_{C1}

$$n_i(\mu_i) \approx \frac{m_w^* k_B T}{\pi \hbar^2} \ln[1 + e^{(\mu_i - \epsilon_{C1})/k_B T}].$$

This yields

$$\mu_i \approx \epsilon_{C1} + k_B T \ln[e^{(\pi \hbar^2 n_i)/m_w^* k_B T} - 1],$$

and therefore

$$\mu_i - \epsilon_{C1} \approx \frac{\pi \hbar^2 n_i}{m_w^*} \quad \text{if } \hbar^2 n_i \gg m_w^* k_B T,$$

$$\mu_i - \epsilon_{C1} \approx k_B T \ln \frac{\pi \hbar^2 n_i}{m_w^* k_B T} \quad \text{if } \hbar^2 n_i \ll m_w^* k_B T.$$

At low temperatures, the chemical potential again depends linearly on the electron density according to Eq. (40), whereas it has ideal-gas logarithmic dependence at high temperatures.

The same considerations used to obtain Eqs. (39) or (41) would indicate that the electron flux across the i th barrier becomes

$$J_{i,i+1} \approx \frac{n_i v_i^{(f)} - n_{i+1} v_i^{(b)}}{d+w},$$

either at low or high enough temperatures. Here $v_i^{(f)}$ and $v_i^{(b)}$ are functions of V_i , $V_{i\pm 1}$. They have dimensions of velocity and correspond to the forward and backward tunneling currents that were invoked in the derivation of phenomenological discrete drift models. When $\epsilon_{w_i} = \epsilon_{w_{i+1}}$, or equivalently, $\mu_{i+1} = \mu_i + eV_i + e(V_{w_i} + V_{w_{i+1}})/2$, $J_{i,i+1} = 0$ according to Eq. (2). Equation (13) implies that $\mu_{i+1} = \mu_i$ if $n_{i+1} = n_i$, and therefore we conclude that $v_i^{(f)} = v_i^{(b)}$ at zero potential drops $V_i + (V_{w_i} + V_{w_{i+1}})/2 = 0$. Notice that $\epsilon_{w_{i+1}} - \epsilon$ becomes $\mu_{i+1} - eV_i - eV_{w_{i+1}}/2 - \epsilon'$ after changing variables in the integral (2). Then $v_i^{(b)}$ is approximately zero unless $0 < \epsilon_{C1} + eV_{w_i}/2 < \mu_{i+1} - eV_i - eV_{w_{i+1}}/2$. For voltages larger than those in the first plateau of the current-voltage characteristic curve this condition does not hold. In fact for these voltages, the level $C1$ of well i is at a higher or equal potential than the level $C2$ of well $i+1$. Then $\epsilon_{C1} \geq \mu_{i+1} - eV_i - e(V_{w_i} + V_{w_{i+1}})/2$.

The previous results yield DDD models with the potential drops at the barriers and the total current density as unknowns, the same as in Eqs. (33)–(38). The main difference with previously used discrete drift models is that the velocity depends on more than one potential drop. To obtain these simpler models, we further assume that $\epsilon V_i/\bar{\epsilon}d$ and $\epsilon V_{i\pm 1}/\bar{\epsilon}d$ are approximately equal to an average field F_i ($\bar{\epsilon}$ is an average permittivity to be chosen later). Then $V_{w_i} = w\bar{\epsilon}F_i/\epsilon_w$ according to Eq. (31). This assumption departs from previous approximations and yields a new model. The point of contact with our previous results is that $A_{C1}(\epsilon)A_{Cj}(\epsilon + eV_i + e[V_{w_i} + V_{w_{i+1}}]/2)$ is the controlling factor in the expressions for $v^{(f)}$ and $v^{(b)}$ (the transmission coefficient contains an exponential factor $e^{-2\alpha_i d}$, which is

almost constant at the energies contributing most to the integral). This controlling factor is uniquely determined by the potential drop

$$V_i + \frac{V_{w_i} + V_{w_{i+1}}}{2} \approx \left(\frac{d}{\epsilon} + \frac{w}{\epsilon_w} \right) \bar{\epsilon} F_i = (d+w) F_i,$$

provided we define the average permittivity as

$$\bar{\epsilon} = \frac{d+w}{\frac{d}{\epsilon} + \frac{w}{\epsilon_w}}. \quad (42)$$

This expression corresponds to the equivalent capacitance of two capacitors in series. Thus the behavior of forward and backward drift velocities is most influenced by the potential drop $V_i + (V_{w_i} + V_{w_{i+1}})/2 \approx F_i(d+w)$ and the new DDD model (see below) should yield results similar to those of the microscopic sequential tunneling model. We have

$$\begin{aligned} J_{i,i+1} &\approx \frac{n_i v^{(f)}(F_i) - n_{i+1} v^{(b)}(F_i)}{d+w} \\ &= \frac{n_i v(F_i)}{d+w} - \frac{n_{i+1} - n_i}{(d+w)^2} D(F_i), \end{aligned} \quad (43)$$

$$v(F) = v^{(f)}(F) - v^{(b)}(F), \quad D(F) = (d+w) v^{(b)}(F). \quad (44)$$

To calculate $v^{(f)}(F)$ and $v^{(b)}(F)$ from $J_{i,i+1}$ in Eq. (2), we replace ϵ_{w_i} , ϵ_{C1}^i , $\epsilon_{w_{i+1}}$ and ϵ_{Cj}^{i+1} by μ_i , ϵ_{C1} , $\mu_{i+1} - e(d+w)F$, and $\epsilon_{Cj} - e(d+w)F$, respectively. The wave vectors in the integrand should be

$$\begin{aligned} \hbar k_i &= \sqrt{2m_w^* \epsilon}, \\ \hbar \alpha_i &= \sqrt{2m^* \left(eV_b - \frac{e w F}{2} - \epsilon \right)}, \\ \hbar k_{i+1} &= \sqrt{2m_w^* [\epsilon + e(d+w)F]}, \\ \hbar \alpha_{i-1} &= \sqrt{2m^* \left[eV_b + e \left(d + \frac{w}{2} \right) F - \epsilon \right]}, \\ \hbar \alpha_{i+1} &= \sqrt{2m^* \left[eV_b - e \left(d + \frac{3w}{2} \right) F - \epsilon \right]}, \end{aligned} \quad (45)$$

and the integration variable ϵ ranges from 0 to ∞ . We substitute $\mu_i(n_i)$ according to Eq. (13) in the result. Then we obtain a function $\mathcal{J}(n_i, n_{i+1}, F)$:

$$\mathcal{J}(n_i, n_{i+1}, F) = \Xi \left(n_i, n_{i+1}, \frac{\bar{\epsilon} F d}{\epsilon}, \frac{\bar{\epsilon} F d}{\epsilon}, \frac{\bar{\epsilon} F d}{\epsilon} \right) \quad (46)$$

[equivalent to setting $V_i = \bar{\epsilon} F d/\epsilon$, or $V_i + (V_{w_i} + V_{w_{i+1}})/2 = (d+w)F$ after transforming this formula to the form (36)]. Notice that (as said above)

$$v^{(f)}(0) = v^{(b)}(0) = \frac{D(0)}{d+w}$$

for the tunneling current to vanish at zero field and equal electron densities at adjacent wells. Furthermore, notice that $D(F)$ vanishes if $\epsilon_{C1} - \mu_{i+1} \geq -e(2V_i + V_{w_i} + V_{w_{i+1}})/2 \approx -e(d+w)F_i$. Thus according to Eq. (40), $D(F)$ vanishes if $\hbar^2 n_{i+1} \leq m_w^* e(d+w)F_i$, which is certainly satisfied for all average fields larger than the first resonant field $(\epsilon_{C2} - \epsilon_{C1})/[e(d+w)]$. In the low-temperature limit (or in the high-temperature limit mentioned earlier in this section, provided it exists), we have

$$\mathcal{J}(n_i, n_{i+1}, F) = \frac{n_i}{d+w} v(F) - \frac{n_{i+1} - n_i}{(d+w)^2} D(F). \quad (47)$$

Then we may use

$$v(F) = \frac{(d+w) \mathcal{J}(N_D^w, N_D^w, F)}{N_D^w}, \quad (48)$$

$$D(F) = - \frac{(d+w)^2 \mathcal{J}(0, N_D^w, F)}{N_D^w} \quad (49)$$

to calculate the drift velocity and the diffusion coefficient from the tunneling current. The integrals from Eq. (2) appearing in these expressions may be approximated by means of the Laplace method: we should just expand their controlling factor mentioned before about its maximum value $\epsilon = \tilde{\epsilon}(F)$. The resulting formulas are cumbersome and we choose not to write them here. We show in the appendix that $v^{(f)}(-F) = v^{(b)}(F) \equiv D(F)/(d+w)$ and $v(-F) = -v(F)$.

Equations (47)–(49) may be used in Eq. (33) to write the Ampère law as

$$\frac{\bar{\epsilon}}{e} \frac{dF_i}{dt} + \frac{n_i v(F_i)}{d+w} - D(F_i) \frac{n_{i+1} - n_i}{(d+w)^2} = J(t) \quad (50)$$

for $i = 1, \dots, N-1$. The Poisson equation (34) becomes

$$F_i - F_{i-1} = \frac{e}{\epsilon} (n_i - N_D^w) \quad (51)$$

for $i = 1, \dots, N$. Equations (50) and (51) constitute a DDD model that may be analyzed on its own together with appropriate bias and boundary conditions. As a bias condition we adopt

$$(d+w) \sum_{i=1}^N F_i = V. \quad (52)$$

Notice that potential drops at the contacts are represented only by the term $F_N(d+w)$. Equation (52) is obtained by inserting $V_i + (V_{w_i} + V_{w_{i+1}})/2 = (w+d)F_i$ into Eq. (26), and omitting

$$(d+w)F_0 + \frac{\Delta_1 + \Delta_2 + 2\epsilon_F}{2e}$$

for the sake of simplicity. For fields higher than the first resonance, $D(F) \approx 0$, and Eq. (50) becomes

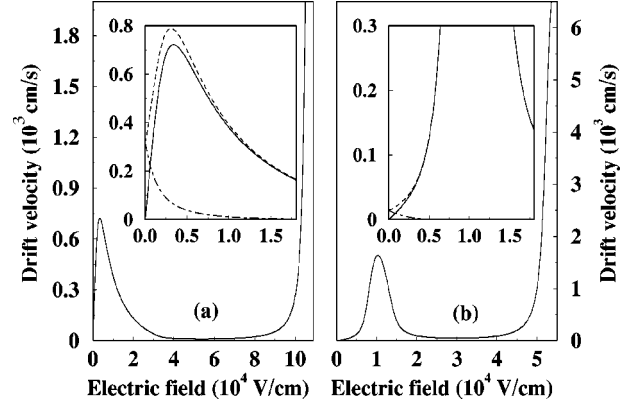


FIG. 2. (a) Electron drift velocity $v(F)$ for the 9/4 SL. Inset: comparison of the drift velocity (continuous line) with the forward (dashed line) and backward (dot-dashed line) velocities. (b) The same for the 13.3/2.7 SL. Notice that the backward velocity or, equivalently the diffusivity, decreases with electric field much more rapidly for this SL.

$$\frac{\bar{\epsilon}}{e} \frac{dF_i}{dt} + \frac{n_i v(F_i)}{d+w} = J(t), \quad (53)$$

which is the usual discrete drift model used in previous theoretical studies.^{15–17}

In Sec. 2.1 of Ref. 13, A. Wacker derived a formula similar to Eq. (43) with $v^{(b)} = 0$ and $v^{(f)}(F) \propto \Gamma / \{ [eF(d+w) + \epsilon_{C1} - \epsilon_{Cj}]^2 + \Gamma^2 \}$, for fields comparable to $(\epsilon_{Cj} - \epsilon_{C1})/[e(d+w)]$. At low fields, the resonant tunneling current between levels $C1$ of adjacent fields was found to be proportional to $W(F) = eF(d+w)/[e^2 F^2 (d+w)^2 + \Gamma_1^2]$ and independent of n_i . While the first approximation of Wacker's (for fields close to higher resonances, $C1 \rightarrow Cj$, $j = 2, 3, \dots$) is compatible with our result (43), the second approximation is an artifact of the extra unnecessary assumption $\epsilon_{w_i} = \epsilon_{w_{i+1}}$.¹³ We shall show in Sec. IV that our drift velocity (48) may have at low fields the same shape as function $W(F)$ for certain SL; see Fig. 2(a). Then the corresponding stationary current for a space homogeneous field profile with $n_i = N_D^w$ (which implies equality of chemical potentials at adjacent fields) will be proportional to $W(F)$ and our result will agree with Wacker's (for this special case). Figure 2(b) shows that things may be different for a different SL configuration.

The boundary conditions for F_0 and F_N are also Ampère's law but now the tunneling currents (1) and (3) (from the emitter and to the collector, respectively) have to be used instead of Eq. (2). The same approximations as before yield

$$\begin{aligned} J_{e,1} &= \Xi_e(n_1, \bar{\epsilon}F_0 d/\epsilon, \bar{\epsilon}F_0 d/\epsilon) \\ &\approx j_e^{(f)}(F_0) - \frac{n_1}{d+w} w^{(b)}(F_0), \end{aligned} \quad (54)$$

$$\begin{aligned} J_{N,c} &= \Xi_c(n_N, \bar{\epsilon}F_N d/\epsilon, \bar{\epsilon}F_N d/\epsilon) \\ &\approx \frac{n_N}{d+w} w^{(f)}(F_N). \end{aligned} \quad (55)$$

Notice that there is no backward tunneling from the collector region to the SL because we are assuming that the potential drop V_N is larger than $\varepsilon_w \epsilon_F d / (e \varepsilon \delta_3)$. Assuming now that Eqs. (54) and (55) are identities, we find

$$j_e^{(f)}(F) = \Xi_e \left(0, \frac{\bar{\varepsilon} F d}{\varepsilon}, \frac{\bar{\varepsilon} F d}{\varepsilon} \right), \quad (56)$$

$$w^{(b)}(F) = \frac{d+w}{N_D^w} \left[j_e^{(f)}(F) - \Xi_e \left(N_D^w, \frac{\bar{\varepsilon} F d}{\varepsilon}, \frac{\bar{\varepsilon} F d}{\varepsilon} \right) \right], \quad (57)$$

$$w^{(f)}(F) = \frac{d+w}{N_D^w} \Xi_c \left(N_D^w, \frac{\bar{\varepsilon} F d}{\varepsilon}, \frac{\bar{\varepsilon} F d}{\varepsilon} \right). \quad (58)$$

The tunneling current across a barrier is zero if the Fermi energies of the adjacent wells are equal. This occurs if the electron density at the first well takes on an appropriate value n_1^w such that the corresponding Fermi energy equals that of the emitter. Then

$$\Xi_e(n_1^w, 0, 0) = 0,$$

and therefore

$$j_e^{(f)}(0) = \frac{n_1^w w^{(b)}(0)}{d+w}.$$

IV. NUMERICAL CALCULATION OF DRIFT VELOCITY AND DIFFUSION

In this section, we shall calculate the functions $v(F)$, $D(F)$, $j_e^{(f)}(F)$, $w^{(b)}(F)$, and $w^{(f)}(F)$ for different SL used in experiments.¹⁷ Figure 2(a) depicts the electron drift velocity $v(F)$ for the $9nm/4nm$ GaAs/AlAs SL (9/4 SL) of Ref. 17 calculated by means of Eq. (48) (at zero temperature; $m^* = m_w^*$ for simplicity). The inset compares $v(F)$ to the backward and forward velocities given by $v^{(b)}(F) = D(F)/(d+w)$ [$D(F)$ as in Eq. (49)] and $v^{(f)}(F) = v(F) + v^{(b)}(F)$. The rapidly decreasing diffusivity $D(F)$ determines the position and height of the first peak in $v(F)$. Notice that $v(F)$ behaves as expected from general considerations: it increases linearly for low-electric fields, it reaches a maximum and then decays before the influence of the second resonance is felt. If $D(F)$ decays faster, a rather different $v(F)$ is found. Figure 2(b) shows $v(F)$ for the 13.3/2.7 SL: there is a wide region before the first peak in which $v''(F) > 0$.

Figures 3 and 4 show the boundary functions $j_e^{(f)}(F)$, $w^{(b)}(F)$, and $w^{(f)}(F)$ for the 9/4 and 13.3/2.7 SL, respectively. Again they behave as expected: (i) the emitter forward current peaks at the resonant values of the electric field [different from those of $v^{(f)}(F)$], (ii) the emitter backward tunnel velocity decreases rapidly with field, and (iii) the collector forward velocity increases monotonically with field given the large difference between the Fermi energies of the last well and the collector.

The emitter forward current $j_e^{(f)}(F)$ is compared in Figs. 5 and 6 to the drift current, $N_D^w v(F)/(d+w)$, for different emitter doping values. Notice that the emitter current is systematically higher than the drift current for large emitter doping at positive electric fields. However, the total current den-

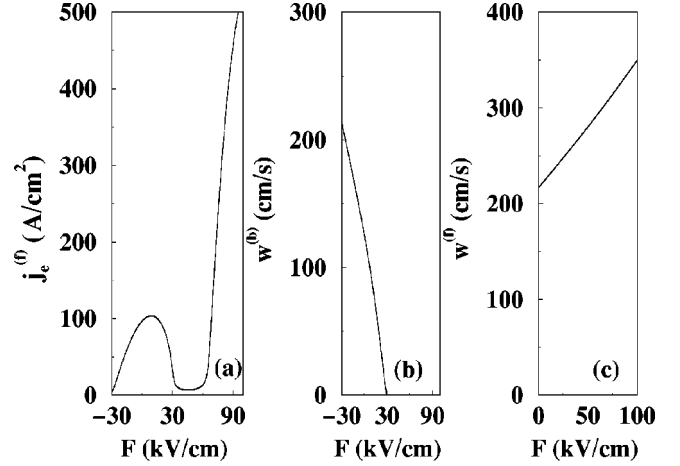


FIG. 3. Functions of the electric field appearing in the boundary conditions for the 9/4 SL with a contact doping $N_D = 2 \times 10^{18} \text{ cm}^{-3}$. (a) $e j_e^{(f)}(F)$ and (b) $w^{(b)}(F)$ for the emitter and (c) $w^{(f)}(F)$ for the collector.

sity should remain between the first maximum and the minimum of the drift current. This means that the contact field F_0 should be negative, so that $j_e^{(f)}(F_0) - n_1 w^{(b)}(F_0)/(d+w) \approx J$, with $n_1 > N_D^w$. Because of Poisson equation (34), F_1 is larger than F_0 and, typically becomes positive. The electric field in the SL increases with distance from the emitter and a charge accumulation layer is formed (see Fig. 5 of Ref. 12 for a similar stationary field profile corresponding to the full microscopic sequential tunneling model). Self-consistent current oscillations in this situation will be due to monopole recycling.¹⁸ Notice that previous work on discrete drift models assumed a fixed excess of electrons in the first SL well as a boundary condition.^{16,17} Again an emitter accumulation layer appeared and monopole self-oscillation resulted.

For smaller emitter doping, $j_e^{(f)}(F)$ intersects $N_D^w v(F)/(d+w)$ on its second branch, and a charge depletion layer may be formed in the SL. Then there may be self-oscillations due to dipole recycling. These findings are

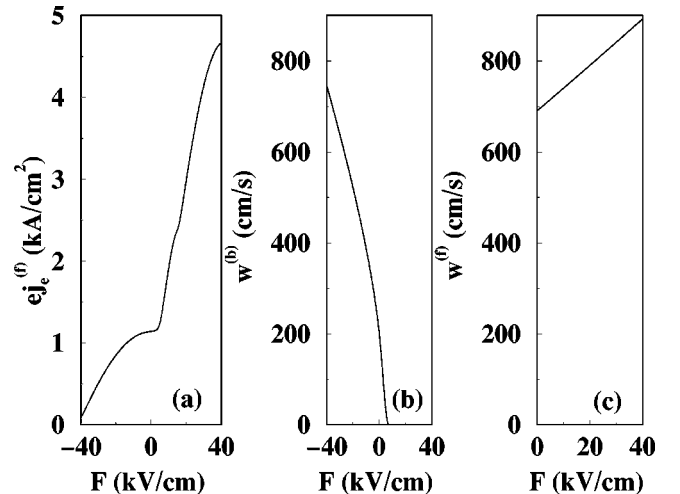


FIG. 4. Same functions as in Fig. 3 for the 13.3/2.7 SL with a contact doping $N_D = 2 \times 10^{18} \text{ cm}^{-3}$. Notice that $e j_e^{(f)}(F)$ is an increasing function since $\epsilon_F > (\epsilon_{C2} - \epsilon_{C1})$ in this SL.

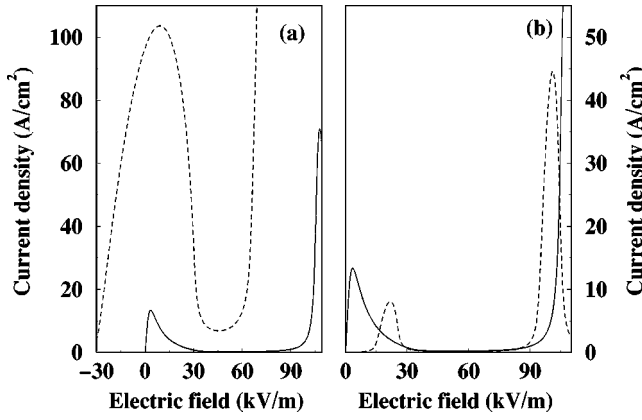


FIG. 5. Comparison of the drift tunneling current density, $eN_D^w v(F)/(d+w)$ (continuous lines) with the emitter current density $e j_e^{(f)}(F)$ (dashed lines) for the 9/4 SL with two different emitter dopings: (a) $N_D = 2 \times 10^{18} \text{ cm}^{-3}$ corresponding to monopole recycling, and (b) $N_D = 2 \times 10^{17} \text{ cm}^{-3}$ corresponding to dipole recycling.

fully consistent with the numerical results reported in Ref. 18 for the 13.3/2.7 SL. That paper reported coexistence and bistability of monopole and dipole self-oscillations. Coexistence and bistability were found for an intermediate emitter doping range (crossover range) *lower* than those used in experiments.¹⁸ A different way to obtain dipole self-oscillations is to decrease the well width without changing contact doping. In this way, we have numerically checked that dipole self-oscillations are possible with emitter doping similar to those used in current experimental setups.¹⁷

For the usual drift-diffusion model of the Gunn effect in bulk n-GaAs, the effect of boundary conditions on the self-oscillations of the current has been well-studied.^{24,25} In particular, asymptotic and numerical calculations for realistic metal-semiconductor contacts were performed some time ago.²⁵ Despite the different equations used in bulk semiconductors, these calculations provide results consistent with our present findings in SL: a boundary condition that yields an accumulation (depletion) layer near injecting contact may yield current self-oscillations due to monopole (dipole) recycling.^{25,24} However these similarities between discrete (SL) and continuous (bulk) drift-diffusion models should not tempt us into reaching hasty conclusions: discrete and continuous drift-diffusion models may have rather different traveling wave solutions.²⁶ In fact, it has been shown that (depending on current and doping), the DDD model may have monopole wave solutions that travel in the same direction as the motion of electrons, in the opposite direction, or remain stationary. In the continuum limit (continuous drift-diffusion model), wavefronts travel always in the same direction as the electrons.²⁶ These features of the DDD equations may have experimentally observable consequences that will be explored elsewhere.

V. CONCLUSIONS

Starting from a microscopic sequential tunneling model of transport in weakly-coupled SL, a DDD model is derived in the limits of low or high temperature. Realistic transport coefficients and contact current-field characteristic curves are

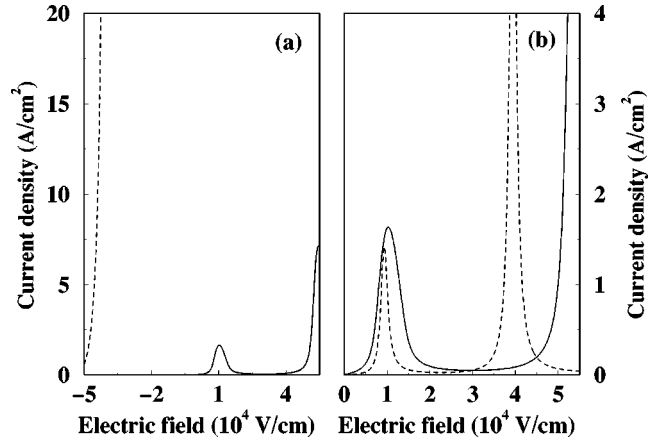


FIG. 6. Same functions as in Fig. 5 for the 13.3/2.7 SL (a) $N_D = 2 \times 10^{18} \text{ cm}^{-3}$ (monopole recycling), and (b) $N_D = 10^{16} \text{ cm}^{-3}$ (dipole recycling).

calculated from microscopic expressions, knowing the design parameters of the superlattice. Boundary conditions select stable spatiotemporal charge or field profiles in the SL. In particular, they clarify when possible self-sustained oscillations of the current are due to monopole or dipole recycling.

ACKNOWLEDGMENTS

One of us (L.L.B.) thanks Dr. Andreas Wacker for fruitful discussions and collaboration on discrete drift-diffusion models. We thank Dr. Ramón Aguado and Dr. Miguel Moscoso for fruitful discussions. This work was supported by the Spanish DGES through Grant Nos. PB98-0142-C04-01 and PB96-0875, by the European Union TMR contracts ERB FMBX-CT97-0157 and FMRX-CT98-0180, and by the Community of Madrid, Project No. 07N/0026/1998.

APPENDIX: MODELS FOR NEGATIVE BIAS

When a negative voltage is applied, we should make sure that our formulas transform appropriately. For negative bias, the charge will be singularly concentrated on planes located at the beginning of the wells. Then we should write

$$\hbar \alpha_i = \sqrt{2m^* \left[eV_b - e \sum_{j=0}^i (V_j + V_{w_j}) - \epsilon \right]},$$

instead of Eq. (6) in expressions (2). The change of variable $\epsilon' = \epsilon + eW_{i+1}$ (i.e., $\epsilon' = 0$ corresponds to zero energy at the bottom of well $i+1$) in the integral (2), then changes the wave vectors to

$$\hbar k_{i+1} = \sqrt{2m_w^* \epsilon},$$

$$\hbar \alpha_i = \sqrt{2m^* \left(eV_b + \frac{eV_{w_{i+1}}}{2} - \epsilon \right)},$$

$$\hbar k_i = \sqrt{2m_w^* \left(\epsilon - eV_i - e \frac{V_{w_i} + V_{w_{i+1}}}{2} \right)},$$

$$\hbar\alpha_{i-1} = \sqrt{2m^* \left(eV_b + eV_{w_i} + eV_i + \frac{eV_{w_{i+1}}}{2} - \epsilon \right)},$$

$$\hbar\alpha_{i+1} = \sqrt{2m^* \left(eV_b - eV_{i+1} - \frac{eV_{w_{i+1}}}{2} - \epsilon \right)}, \quad (\text{A1})$$

instead of Eq. (15).

Given the new location of the singular charge planes (at the beginning of wells), Eq. (20) still holds, but Eq. (21) should be replaced by

$$\frac{V_{w_i}}{w} = \frac{V_{w_{i-1}}}{w} + \frac{e(n_i - N_D^w)}{\epsilon_w}. \quad (\text{A2})$$

Then we find

$$\frac{\epsilon V_i}{\epsilon_w d} = \frac{V_{w_i} + V_{w_{i+1}}}{2w}, \quad (\text{A3})$$

instead of Eq. (31). Inserting this equation in the functions $\tilde{\Xi}$ (tunneling current under negative bias), we obtain new functions $\Xi^*(n_i, n_{i+1}, V_{w_i}, V_{w_{i+1}}, V_{w_{i+2}})$, instead of $\Xi(n_i, n_{i+1}, V_{i-1}, V_i, V_{i+1})$ valid for positive voltage. To obtain a reduced model, we now set

$$\epsilon_{C1}^i = \epsilon_{C1} + e(d+w)F,$$

$$\epsilon_{Cj}^{i+1} = \epsilon_{Cj},$$

$$\epsilon_{w_i} = \mu_i + e(d+w)F,$$

$$\epsilon_{w_{i+1}} = \mu_{i+1},$$

$$\hbar k_{i+1} = \sqrt{2m_w^* \epsilon},$$

$$\hbar\alpha_i = \sqrt{2m^* \left(eV_b + \frac{ewF}{2} - \epsilon \right)},$$

$$\hbar k_i = \sqrt{2m_w^* [\epsilon - e(d+w)F]},$$

$$\hbar\alpha_{i-1} = \sqrt{2m^* \left[eV_b + e \left(d + \frac{3w}{2} \right) F - \epsilon \right]},$$

$$\hbar\alpha_{i+1} = \sqrt{2m^* \left[eV_b - e \left(d + \frac{w}{2} \right) F - \epsilon \right]}, \quad (\text{A4})$$

in the integrals (2) and let the variable of integration ϵ range from 0 to ∞ . This is equivalent to setting V_{w_i} , $V_{w_{i+1}}$, and $V_{w_{i+2}}$ equal to $\bar{\epsilon}wF/\epsilon_w$ in $\Xi^*(n_i, n_{i+1}, V_{w_i}, V_{w_{i+1}}, V_{w_{i+2}})$. Equations (2), (45), and (A4) and the previous definitions in this appendix imply

$$\Xi \left(n_i, n_{i+1}, \frac{\bar{\epsilon}Fd}{\epsilon}, \frac{\bar{\epsilon}Fd}{\epsilon}, \frac{\bar{\epsilon}Fd}{\epsilon} \right)$$

$$= -\Xi^* \left(n_{i+1}, n_i, -\frac{\bar{\epsilon}Fw}{\epsilon_w}, -\frac{\bar{\epsilon}Fw}{\epsilon_w}, -\frac{\bar{\epsilon}Fw}{\epsilon_w} \right). \quad (\text{A5})$$

The Poisson equation (A2) still yields Eq. (51). Notice that the symmetry (A5) implies

$$v^{(f)}(-F) = v^{(b)}(F) \equiv \frac{D(F)}{d+w}, \quad v(-F) = -v(F). \quad (\text{A6})$$

Given the difference between the states at the contact regions and the wells, the previous arguments cannot be used to extend the contact current-field characteristic curves to negative fields. Direct calculation of Eqs. (56)–(58) by means of Eqs. (1) and (3) yields the results depicted in Figs. 3 and 4.

¹L. P. Kadanoff and G. Baym, *Quantum Statistical Mechanics* (Benjamin, New York, 1962); L. V. Keldysh, Zh. Éksp. Theor. Fiz **47**, 1515 (1964) [Sov. Phys. JETP **20**, 1018 (1965)].

²H. Haug and A.-P. Jauho, *Quantum Kinetics in Transport and Optics of Semiconductors* (Springer-Verlag, Berlin, 1996).

³A. Wacker and A.-P. Jauho, Phys. Rev. Lett. **80**, 369 (1998).

⁴A. Wacker, A.-P. Jauho, S. Rott, A. Markus, P. Binder, and G. H. Döhler, Phys. Rev. Lett. **83**, 836 (1999).

⁵J. F. Palmier, G. Etemadi, A. Sibille, M. Hadjazi, F. Mollot, and R. Planel, Surf. Sci. **267**, 574 (1992); R. R. Gerhardts, Phys. Rev. B **48**, 9178 (1993); A. A. Ignatov, E. P. Dodin, and V. I. Shashkin, Mod. Phys. Lett. B **5**, 1087 (1991).

⁶M. Büttiker and H. Thomas, Phys. Rev. Lett. **38**, 78 (1977); Z. Phys. B **34**, 301 (1979); X. L. Lei, N. J. M. Horing, and H. L. Cui, Phys. Rev. Lett. **66**, 3277 (1991); J. C. Cao and X. L. Lei, Phys. Rev. B **60**, 1871 (1999).

⁷A. Sibille, J. F. Palmier, F. Mollot, H. Wang, and J. C. Esnault, Phys. Rev. B **39**, 6272 (1989).

⁸L. Esaki and R. Tsu, IBM J. Res. Dev. **14**, 61 (1970).

⁹J. B. Gunn, Solid State Commun. **1**, 88 (1963).

¹⁰R. Tsu and G. H. Döhler, Phys. Rev. B **12**, 680 (1975); S. Rott, N. Linder, and G. H. Döhler, Superlattices Microstruct. **21**, 569 (1997); S. Rott, P. Binder, N. Linder, and G. H. Döhler, Phys. Rev. B **59**, 7334 (1999).

¹¹R. F. Kazarinov and R. A. Suris, Fiz. Tekh. Poluprov. **6**, 148 (1972) [Sov. Phys. Semicond. **6**, 120 (1972)].

¹²R. Aguado, G. Platero, M. Moscoso, and L. L. Bonilla, Phys. Rev. B **55**, R16 053 (1997).

¹³A. Wacker, in *Theory and Transport Properties of Semiconductor Nanostructures*, edited by E. Schöll (Chapman and Hill, New York, 1998), Chap. 10.

¹⁴F. Prengel, A. Wacker, and E. Schöll, Phys. Rev. B **50**, 1705 (1994).

¹⁵L. L. Bonilla, J. Galán, J. A. Cuesta, F. C. Martínez, and J. M. Molera, Phys. Rev. B **50**, 8644 (1994).

¹⁶L.L. Bonilla, in *Nonlinear Dynamics and Pattern Formation in Semiconductors and Devices*, edited by F.-J. Niedernostheide (Springer-Verlag, Berlin, 1995), pp. 1–20; A. Wacker, M.

- Moscoso, M. Kindelan, and L. L. Bonilla, *Phys. Rev. B* **55**, 2466 (1997); L. L. Bonilla, M. Kindelan, M. Moscoso, and S. Venakides, *SIAM J. Appl. Math.* **57**, 1588 (1997).
- ¹⁷J. Kastrup, H. T. Grahn, R. Hey, K. Ploog, L. L. Bonilla, M. Kindelan, M. Moscoso, A. Wacker, and J. Galán, *Phys. Rev. B* **55**, 2476 (1997); J. W. Kantelhardt, H. T. Grahn, K. H. Ploog, M. Moscoso, A. Perales, and L. L. Bonilla, *Phys. Status Solidi B* **204**, 500 (1997).
- ¹⁸D. Sánchez, M. Moscoso, L. L. Bonilla, G. Platero, and R. Aguado, *Phys. Rev. B* **60**, 4489 (1999).
- ¹⁹T. Weil and B. Vinter, *Appl. Phys. Lett.* **50**, 1281 (1987).
- ²⁰R. Aguado and G. Platero, *Phys. Rev. B* **55**, 12 860 (1997).
- ²¹R. Aguado and G. Platero, *Superlattices Microstruct.* **22**, 9 (1997).
- ²²G. Platero and R. Aguado, *Appl. Phys. Lett.* **70**, 3546 (1997).
- ²³V. J. Goldman, D. C. Tsui, and J. E. Cunningham, *Phys. Rev. Lett.* **58**, 1256 (1987); *Phys. Rev. B* **35**, 9387 (1987); J. Iñarrea and G. Platero, *Europhys. Lett.* **33**, 477 (1996).
- ²⁴M. P. Shaw, H. L. Grubin, and P. R. Solomon, *The Gunn-Hilsum Effect* (Academic, New York, 1979).
- ²⁵G. Gomila, J. M. Rubí, I. R. Cantalapiedra, and L. L. Bonilla, *Phys. Rev. E* **56**, 1490 (1997); L. L. Bonilla, I. R. Cantalapiedra, G. Gomila, and J. M. Rubí, *ibid.* **56**, 1500 (1997).
- ²⁶A. Carpio, L. L. Bonilla, A. Wacker, and E. Schöll, *Phys. Rev. E* **61**, 4866 (2000).